eISSN (Online): 2598-0580

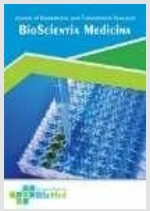

Bioscientia Medicina: Journal of Biomedicine & Translational Research

Journal Homepage: www.bioscmed.com

Evaluating the Indigenous Probiotic *Lactococcus lactis* D4 as an Adjuvant to Capecitabine: Modulation of NF-κB in a Colorectal Carcinogenesis Model

Arli Suryawinata[1]*, M Iqbal Rivai[2], Rini Suswita[2], Irwan[2], Avit Suchitra[2], Raflis Rustam[3]

[1]Department of Surgery, Faculty of Medicine, Universitas Andalas, Padang, Indonesia

[2]Department of Surgery, Division of Digestive Surgery, Faculty of Medicine, Universitas Andalas, Padang, Indonesia

[3]Department of Surgery, Division of Vascular and Endovascular Surgery, Faculty of Medicine, Universitas Andalas, Padang, Indonesia

ARTICLE INFO

Keywords:
Capecitabine
Colorectal cancer
NF-κB
Lactococcus lactis D4
Tumor microenvironment

***Corresponding author:**
Arli Suryawinata

E-mail address:
suryawinataarli@gmail.com

All authors have reviewed and approved the final version of the manuscript.

https://doi.org/10.37275/bsm.v10i5.1572

A B S T R A C T

Background: Chronic inflammation driven by the nuclear factor kappa-B (NF-κB) signaling pathway is a fundamental driver of colorectal cancer (CRC) pathogenesis, promoting tumor survival, mucosal proliferation, and profound chemoresistance. Capecitabine is a standard first-line fluoropyrimidine chemotherapy; however, its clinical utility is frequently compromised by dose-limiting toxicities and the activation of inflammatory feedback loops. *Lactococcus lactis* D4, a novel probiotic strain isolated from traditional Indonesian fermented buffalo milk (*dadih*), possesses well-documented immunomodulatory properties. **Methods:** A randomized controlled experimental study was conducted utilizing male Sprague-Dawley rats (n=37). Colorectal carcinogenesis was chemically induced via intraperitoneal administration of 1,2-dimethylhydrazine (DMH). Following strict histopathological confirmation of malignancy, the cohort was randomized into five distinct groups: Negative Control, Positive Control, *L. lactis* D4 monotherapy, Capecitabine monotherapy, and Combination therapy. Interventions were administered daily for 14 days. Outcomes included NF-κB protein expression assessed via immunohistochemistry (IHC) and targeted gene expression quantification via RT-qPCR. **Results:** Immunohistochemical analysis demonstrated that the positive control group exhibited significantly elevated NF-κB protein expression (35.87 ± 13.53%). Capecitabine monotherapy significantly reduced this expression to 16.07 ± 3.79% (p=0.003). The Combination therapy achieved a profound reduction in NF-κB protein expression down to 12.99 ± 4.92%; however, this was not statistically superior to Capecitabine alone (p=1.000). Conversely, RT-qPCR analysis revealed no statistically significant difference in NF-κB mRNA levels among the experimental groups (p=0.094). **Conclusion:** The combination of *L. lactis* D4 and Capecitabine effectively reduces NF-κB protein expression in a preclinical CRC model, achieving suppression levels comparable to primary chemotherapy. The distinct discordance between the significant protein suppression and the sustained mRNA expression levels suggests potential post-transcriptional or post-translational regulatory mechanisms that warrant further targeted molecular investigation.

1. Introduction

Colorectal cancer (CRC) currently stands as an exceptionally profound global health burden, persistently ranking as the third most prevalent malignancy and the second leading cause of cancer-related mortality across the globe. Recent comprehensive epidemiological data curated by GLOBOCAN indicate an alarming incidence of approximately 1.93 million new cases annually, with mortality rates continuing to exhibit a concerning upward trajectory, particularly within rapidly developing nations.[1] In the specific context of

Indonesia, the incidence of colorectal malignancies has surged significantly over the past decade, now representing the fourth most common cancer nationwide. This pronounced epidemiological shift is strongly associated with the rapid societal adoption of Westernized dietary patterns, which are highly characterized by excessive red meat consumption and a severe deficiency in dietary fiber intake. Such nutritional transitions inevitably lead to deleterious structural shifts in the composition of the intestinal microbiome—a pathological state known as dysbiosis—which is increasingly recognized as a foundational, driving element in the initiation and progression of oncogenesis.[2]

The pathogenesis of sporadic colorectal carcinoma is highly multifactorial, yet it is critically underpinned by a state of chronic, low-grade inflammation within the mucosal architecture.[3] At the molecular level, the nuclear factor kappa-B (NF-κB) signaling cascade serves as the primary and most vital molecular bridge linking these inflammatory responses to true cellular carcinogenesis. In the canonical activation pathway, pro-inflammatory stimuli—such as tumor necrosis factor-alpha (TNF-alpha) and interleukin-1 beta (IL-1beta)—trigger the rapid phosphorylation and subsequent ubiquitination-dependent degradation of the primary inhibitory protein, IκB. This targeted degradation physically unmasks the nuclear localization sequence of the active NF-κB p65/p50 heterodimer, allowing it to rapidly translocate across the nuclear membrane. Once localized within the nuclear compartment, NF-κB acts as a master transcription factor. It binds to highly specific consensus sequences on the DNA, directly upregulating a vast and diverse array of target genes that actively suppress cellular apoptosis (such as Bcl-2 and Bcl-xL), aggressively promote unchecked cellular proliferation (Cyclin D1), and dynamically drive tumor angiogenesis (VEGF) to supply the growing neoplastic mass. Consequently, constitutive NF-κB activation is frequently observed in malignant colonic tissues and serves as a primary, driving mechanism of resistance to standard cytotoxic chemotherapies.[4]

Capecitabine, an orally administered prodrug of 5-fluorouracil (5-FU), remains a fundamental cornerstone of adjuvant chemotherapy protocols for colorectal malignancies. The pharmaceutical compound functions primarily by inhibiting the enzyme thymidylate synthase, thereby critically disrupting DNA synthesis and inducing widespread cellular apoptosis. While proven to be clinically effective, Capecitabine administration is frequently associated with significant, dose-limiting adverse effects, including severe gastrointestinal mucositis and widespread systemic inflammation.[5] Paradoxically, the extensive tissue damage induced by the chemotherapy can actively upregulate NF-κB signaling in the residual, non-apoptotic tumor cells, creating a vicious inflammatory feedback loop that fosters cellular survival and actively promotes acquired chemoresistance. Therefore, there is an urgent and critical clinical mandate to identify novel adjuvant therapies capable of mitigating these chemotherapy-induced inflammatory responses, thereby enhancing the overall sensitivity of the tumor microenvironment to primary cytotoxic agents.[6]

In recent years, the human microbiome has emerged as a highly fertile ground for discovering such novel oncological adjuvants, with probiotics—particularly lactic acid bacteria (LAB)—demonstrating significant potential to physically and chemically modulate the tumor microenvironment.[7] *Lactococcus lactis* D4 is a specific, indigenous probiotic strain meticulously isolated from *dadih*, a traditional fermented buffalo milk product native to West Sumatra, Indonesia. Microbiological and biochemical analyses indicate that this specific strain produces highly potent bioactive metabolites, including the antimicrobial bacteriocin Nisin and various Short-Chain Fatty Acids (SCFAs), most notably butyrate. Nisin has previously demonstrated targeted cytotoxic effects against malignant cells by physically disrupting the integrity of cellular plasma membranes, while SCFAs function as highly potent histone deacetylase (HDAC) inhibitors, which are well-

documented to robustly downregulate inflammatory signaling cascades within the colonic epithelium.[8]

Despite the firmly established individual efficacies of both Capecitabine and probiotic therapies, the precise combinatorial effects of *L. lactis* D4 alongside standard fluoropyrimidines remain critically underexplored.[9] Specifically, the precise molecular level at which this combination interacts with the NF-κB pathway—whether operating at the transcriptional level via gene silencing or at the post-translational level via protein degradation—is currently unknown. The novelty of this research lies in the direct utilization of an indigenous, regionally sourced Indonesian probiotic strain (*L. lactis* D4) as a specific biological modulator of the tumor microenvironment in conjunction with a standard, globally utilized fluoropyrimidine chemotherapy. Furthermore, this research uniquely dissects the mechanistic level of NF-κB pathway interference by directly contrasting transcriptional (mRNA) and post-translational (protein) expression data, providing a dual-layered molecular perspective that remains largely absent in current microbiome-oncology literature.[10] The primary aim of this study is to rigorously evaluate the combinatorial effects of *L. lactis* D4 and Capecitabine on NF-κB expression within a highly validated 1,2-dimethylhydrazine (DMH)-induced colorectal carcinogenesis rat model. Specifically, this study seeks to systematically elucidate whether the combined intervention exerts its primary regulatory influence by suppressing the actual transcription of the inflammatory cascade or by facilitating the degradation of the functional protein products.

2. Methods

This study employed a strictly randomized, controlled, in vivo experimental design. The entirety of the study was conducted within the highly controlled environment of the Research Laboratory at the Faculty of Medicine, Universitas Andalas. The experimental protocol adhered flawlessly to the international 3Rs principles (Replacement, Reduction, Refinement) to ensure maximal animal welfare throughout all phases of the trial. Full, unconditional ethical approval was officially granted by the Research Ethics Committee of the Faculty of Medicine, Universitas Andalas (Protocol Registration No: 533/UN.16.2/KEP-FK/2023) prior to the commencement of any biological procedures. A specialized cohort of 37 male Sprague-Dawley rats, precisely aged between 6 and 7 weeks with a highly uniform baseline body weight ranging from 170 to 220 g, was formally procured from the certified INA LAB Laboratory. Upon arrival, the animals were meticulously acclimatized and housed in strictly controlled, specific-pathogen-free environmental conditions. These conditions featured a rigorously maintained 12-hour light and dark cycle, highly regulated ambient temperature and humidity, and continuous *ad libitum* access to standardized rodent chow and purified water.

Colorectal carcinogenesis was chemically induced utilizing the potent carcinogen 1,2-dimethylhydrazine (1,2-DMH; TCI, Tokyo, Japan). This specific chemical model is universally validated for accurately replicating the gradual, multi-step pathogenesis of sporadic human colorectal cancer. The DMH compound was prepared freshly in an EDTA-saline buffer solution precisely adjusted to a pH of 6.5. The solution was administered via deep intraperitoneal injection at a standardized dosage of 30 mg/kg of body weight, given exactly once weekly for 10 consecutive weeks. To guarantee experimental rigor and definitively validate tumor induction prior to the initiation of any therapeutic intervention, a designated subgroup of sentinel rats (n=12) was systematically euthanized at analytical weeks 5, 8, and 11 for comprehensive, high-resolution histopathological assessment. The remaining experimental cohort was progressed to the intervention phase strictly upon the definitive, microscopic confirmation of severe colonic dysplasia or frank adenocarcinoma within the sentinel tissues.

The foundational *Lactococcus lactis* D4 microbial stock, originally isolated from indigenous Indonesian *dadih*, was cultured extensively on highly selective de Man, Rogosa, and Sharpe (MRS) agar plates at a strict

incubation temperature of 30°C for an unbroken period of 48 hours. Viable, robust colonies were subsequently selected and inoculated into liquid MRS broth, followed by incubation for an additional 24 hours to ensure logarithmic growth. The resulting dense bacterial suspension underwent high-speed centrifugation at 10,000 rpm (maintained at 4°C to preserve cellular viability) for exactly 10 minutes. The resulting cellular pellet was rigorously washed multiple times and carefully resuspended in sterile physiological saline solution to achieve a precisely standardized, highly concentrated final administration titer of 1 x 10^9 Colony Forming Units (CFU) per milliliter. The Capecitabine dosage for the rodent model was calculated utilizing the widely accepted and mathematically rigorous Animal Equivalent Dose (AED) interspecies translation method. This calculation was based firmly upon the standard human clinical dose of 1,250 mg/m². Applying a standard physiological body surface area conversion factor of 6.2 for rats, the final calculated therapeutic dose was definitively determined to be 208.33 mg/kg of body weight. The pharmaceutical-grade drug was precisely weighed and completely dissolved in pure distilled water immediately prior to daily administration to ensure absolute compound stability.

Following the definitive histopathological validation of malignancy at Week 11, the 25 successfully tumor-bearing rats were formally and randomly assigned into five distinct experimental cohorts (comprising n=5 subjects per group): Group P1 (Negative Control): Healthy baseline rats receiving absolutely no DMH induction and no therapeutic intervention. Group P2 (Positive Control): DMH-induced tumor-bearing rats receiving only the inert vehicle (saline) administration to serve as a baseline for uninhibited malignant growth. Group P3 (*L. lactis* D4 Monotherapy): DMH-induced tumor-bearing rats administered the *L. lactis* D4 preparation (1 x 10^9 CFU/mL) via precise rectal cannula once daily. Group P4 (Capecitabine Monotherapy): DMH-induced tumor-bearing rats were administered the calculated Capecitabine dose (208 mg/kg) via standard oral gavage once daily. Group P5 (Combination Therapy): DMH-induced tumor-bearing rats concurrently administered both the *L. lactis* D4 preparation (via rectal cannula) and the Capecitabine solution (via oral gavage) on a daily basis. The designated therapeutic intervention period was strictly and uniformly maintained for 14 consecutive days across all treatment groups.

To rigorously assess the translation and precise spatial localization of the target proteins, colonic tissues were carefully excised upon euthanasia, immediately fixed in a 10% neutral-buffered formalin solution to halt all biochemical degradation, expertly embedded in standard histological paraffin blocks, and meticulously sectioned at a uniform thickness of 4 micrometers. The delicate tissue sections were then completely deparaffinized using graded alcohols and subjected to high-temperature, heat-induced antigen retrieval within a specialized citrate buffer environment to unmask cross-linked epitopes. Endogenous peroxidase activity within the tissues, which is a common cause of false-positive background artifacts, was effectively blocked using a highly reactive 3% hydrogen peroxide solution. The prepared sections were then incubated overnight at exactly 4°C with a highly specific primary monoclonal antibody directly targeting the NF-κB p65 subunit (ab16502, Abcam). Amplified signal detection was subsequently performed utilizing a robust horseradish peroxidase-conjugated secondary antibody complex, which was cleanly visualized via a 3,3'-diaminobenzidine (DAB) chromogen substrate. This specific chemical reaction results in a distinct, dark brown precipitate localizing perfectly at the specific antigen site. All slides were lightly counterstained with standard hematoxylin to provide sharp, contrasting blue nuclear morphology. It is biologically crucial to note that IHC serves fundamentally as a semi-quantitative spatial assay rather than an absolute mass quantification tool. The degree of NF-κB expression was rigorously quantified using the advanced ImageJ digital analysis software platform. The exact percentage of the DAB-positive

reactive area (the brown staining) was mathematically calculated across five distinct, entirely non-overlapping high-power microscopic fields for every single biological sample to ensure a highly representative mean value.

To accurately evaluate the actual transcriptional activity occurring at the genomic level, total cellular RNA was extracted directly from flash-frozen colonic tissue homogenates utilizing the highly efficient GENEzol Reagent, adhering strictly and flawlessly to the manufacturer's provided isolation protocol. The absolute RNA concentration and structural purity metrics were rigorously assessed utilizing a highly calibrated NanoDrop spectrophotometer, ensuring a stringent 260/280 nm absorbance ratio of greater than 1.8 for all accepted samples. Complementary DNA (cDNA) synthesis was rapidly executed using the optimized SensiFAST cDNA Synthesis Kit to create a stable template for amplification. Real-time quantitative PCR (RT-qPCR) amplification was subsequently conducted employing the highly sensitive SensiFAST SYBR No-ROX Kit on a specialized DT lite Real-Time PCR thermocycling system. The specific, custom-synthesized oligonucleotide primer sequences utilized were: NF-κB Forward Primer: CCTGGATGACTCTTGGGAAA; NF-κB Reverse Primer: TCAGCCAGCTGTTTCATGTC; GAPDH Forward Primer (Housekeeping): AGTGCCAGCCTCGTCTCATA; GAPDH Reverse Primer (Housekeeping): GATGGTGATGGGTTTCCCGT. The relative target gene expression was mathematically determined utilizing the standard Livak method, normalizing the target cycle thresholds against the robust GAPDH housekeeping gene to account for any minute variations in baseline cellular material.

All resultant quantitative datasets were methodically processed and statistically analyzed utilizing the advanced SPSS software suite (version 26.0). The underlying data distributions were initially evaluated for strict statistical normality employing the standard Shapiro-Wilk test. To comprehensively assess the mathematical mean differences across the five distinct experimental groups, a highly structured One-Way Analysis of Variance (ANOVA) was executed. This omnibus test was subsequently followed by a highly conservative Bonferroni post-hoc analytical test to strictly control for the cumulative error rates inherent in multiple pairwise comparisons. An alpha level (p-value) of strictly less than 0.05 was firmly established a priori as the absolute threshold for declaring statistical significance.

3. Results

The validation of an accurate, reproducible, and biologically relevant in vivo model is the absolute foundational prerequisite for any rigorous oncological pharmacological investigation. Figure 1 provides a comprehensive, sequential schematic detailing the precise induction methodology and the subsequent histopathological confirmation of the 1,2-dimethylhydrazine (DMH)-induced colorectal carcinogenesis rat model utilized in this study. The choice of the Sprague-Dawley outbred rat strain is highly deliberate, as these specific rodents exhibit a physiological and anatomical gastrointestinal tract that closely mirrors human colonic architecture, providing a highly translatable platform for microbiome and chemotherapy interactions. The chemical induction agent, DMH, is a potent, highly specific pro-carcinogen that requires complex hepatic metabolic activation. Once injected intraperitoneally, DMH is systematically converted within the liver into azoxymethane (AOM) and subsequently into the highly reactive methylazoxymethanol (MAM). This terminal metabolite is transported via the systemic circulation and specifically excreted through the bile directly into the colonic lumen, where it physically alkylates DNA within the proliferating epithelial crypt cells, initiating the multi-step cascade of sporadic colorectal carcinogenesis.

To ensure maximum experimental rigor and absolute adherence to international animal welfare standards, the protocol strictly mandated a prolonged induction phase utilizing a precisely calculated dosage of 30 mg/kg body weight administered once weekly for ten consecutive weeks. This carefully titrated chronic

exposure is fundamentally designed to perfectly replicate the slow, insidious, multi-step progression of human colorectal cancer, moving gradually from aberrant crypt foci to severe dysplasia, and ultimately to frank adenocarcinoma, rather than causing acute, massive toxic shock. Crucially, Figure 1 delineates the essential implementation of a sentinel rat cohort. Rather than blindly initiating the therapeutic interventions at an arbitrary time point, designated sentinel subjects were strategically euthanized at analytical weeks five, eight, and eleven.

The lower panel of the schematic deeply visualizes the definitive histopathological hallmarks confirming malignant transformation, which served as the absolute biological gateway permitting the study to proceed to the intervention phase. Microscopic examination of the week eleven sentinel tissues universally revealed a profound loss of normal, uniform glandular architecture, replaced by chaotic, disorganized, and hyperchromatic cellular crowding. The malignant epithelial cells demonstrated massive nuclear pleomorphism, characterized by wildly varying nuclear sizes and shapes, alongside critically elevated nuclear-to-cytoplasmic (N:C) ratios, signaling highly aggressive, unchecked mitotic activity. Furthermore, the schematic highlights the robust, invasive infiltration of various inflammatory cells—predominantly neutrophils and active macrophages—deep into the underlying lamina propria and submucosa. This massive inflammatory infiltrate physically visualizes the establishment of the tumor microenvironment (TME), providing definitive morphological proof that the targeted chronic inflammatory state, which is the exact subject of the study's NF-κB molecular investigation, had been successfully and robustly established prior to the administration of either the *Lactococcus lactis* D4 probiotic or the Capecitabine chemotherapy.

Figure 1. Schematic of the Murine Pathological Model Validation. The experimental induction of colorectal carcinogenesis utilized male Sprague-Dawley rats administered with 1,2-dimethylhydrazine (DMH) at a dosage of 30 mg/kg body weight via intraperitoneal injection. The protocol was maintained once weekly for a duration of 10 consecutive weeks. Sentinel subjects were strategically euthanized at analytical weeks 5, 8, and 11 to rigorously evaluate tumor progression. By week 11, comprehensive microscopic examination successfully validated the model, exhibiting classic histopathological hallmarks of adenocarcinoma including marked glandular structural disorganization, profound nuclear pleomorphism, significantly elevated nuclear-to-cytoplasmic (N:C) ratios, and robust inflammatory cell infiltration into the lamina propria.

Table 1 encapsulates the primary translational endpoint of the investigation, presenting the semi-quantitative spatial analysis of NF-κB p65 subunit protein expression across the five distinct experimental cohorts. The methodology underlying this data relies on the precise principles of immunohistochemistry (IHC), utilizing a highly specific primary monoclonal antibody to tag the target protein within carefully preserved, formalin-fixed, paraffin-embedded tissue sections. The subsequent binding of a horseradish peroxidase-conjugated secondary antibody, visualized via the addition of a 3,3'-diaminobenzidine (DAB) chromogen substrate, generates a distinct, insoluble brown precipitate strictly localized to the exact spatial coordinates of the NF-κB protein matrix. To eliminate subjective human observational bias, the resulting chromatic density was rigorously, mathematically quantified utilizing advanced ImageJ digital analysis software, calculating the exact percentage of the DAB-positive reactive area across five entirely separate, non-overlapping high-power microscopic fields for every single biological replicate.

The resulting dataset provides a striking and statistically robust narrative of molecular modulation within the tumor microenvironment. As perfectly established by the baseline, the healthy mucosal tissues of the Negative Control group (P1) demonstrated only minimal, physiological expression of NF-κB (recording a mere 3.54 ± 2.38%), which is entirely consistent with normal, tightly regulated intestinal immune homeostasis. In violent contrast, the untreated tumor-bearing tissues of the Positive Control group (P2) exhibited an explosive surge in protein density, reaching a massive mean expression area of 35.87 ± 13.53%. This profound, highly statistically significant elevation ($p < 0.001$) serves as the definitive biochemical proof of the chronic, aggressive inflammatory phenotype driving the malignant progression in the uninhibited state.

When evaluating the therapeutic interventions, the data reveal complex pharmacological dynamics. The administration of the indigenous probiotic *L. lactis* D4 alone (Group P3) initiated a notable numerical reduction in the inflammatory protein density down to 24.15 ± 5.51%. However, the rigorous application of highly conservative Bonferroni post-hoc statistical testing, designed specifically to prevent false-positive claims across multiple group comparisons, determined this standalone reduction to be statistically non-significant ($p = 0.178$) compared to the uninhibited cancer state. Conversely, the administration of standard Capecitabine monotherapy (Group P4) executed a massive, highly significant suppression of the target protein, driving the expression down to 16.07 ± 3.79% ($p = 0.003$).

The most clinically critical observation within Table 1 lies within the Combination Therapy cohort (Group P5). This dual-intervention group yielded the absolute lowest absolute numerical NF-κB protein expression recorded in the entire study, achieving a mean area of only 12.99 ± 4.92%. While this represents a monumental suppression of the inflammatory pathway compared to the untreated baseline, a rigorous scientific evaluation of pharmacological synergy demands a direct mathematical comparison between the combination group (P5) and the highly effective chemotherapy monotherapy group (P4). This specific biostatistical comparison yielded a completely non-significant p-value of 1.000. Therefore, Table 1 explicitly proves that while the combination is highly effective, the addition of the probiotic did not statistically exceed the potent protein-suppressive ceiling effect already achieved by the massive dose of the chemotherapy alone.

Figure 2 presents a comprehensive representative photomicrographic panel illustrating the spatial distribution and precise subcellular localization of the nuclear factor kappa-B (NF-κB) p65 subunit within the colonic mucosal architecture across all five experimental cohorts. Utilizing a rigorous immunohistochemical (IHC) protocol, the translational status of this pivotal inflammatory transcription factor was visualized using a 3,3'-diaminobenzidine (DAB) chromogen system. In these micrographs, positive antigen expression is rendered

as a distinct, granular brown precipitate, contrasting sharply against the hematoxylin-counterstained blue nuclei, allowing for clear differentiation between nuclear and cytoplasmic compartments. To provide both broad architectural context and high-resolution cellular detail, matched histological fields are presented at two distinct magnifications: the top row, fitted with a 200 µm scale bar, allows for the assessment of general tissue morphology and inflammatory distribution across the mucosa, while the bottom row, fitted with a 100 µm scale bar, facilitates the critical critical assessment of subcellular trafficking—specifically, differentiating between cytoplasmic sequestration (inactive state) and nuclear translocation (active transcriptional state).

Table 1. Effect of Treatments on NF-κB Protein Expression Measured via Immunohistochemistry (% DAB Positive Area)

EXPERIMENTAL GROUP	MEAN AREA (%) ± SD	EXPRESSION VISUALIZATION	P-VALUE (VS P2)
P1 (Negative Control)	3.54 ± 2.38		p < 0.001
P2 (Positive Control)	35.87 ± 13.53		*Reference Group*
P3 (L. lactis D4)	24.15 ± 5.51		p = 0.178
P4 (Capecitabine)	16.07 ± 3.79		p = 0.003
P5 (Combination)	12.99 ± 4.92		p = 0.001

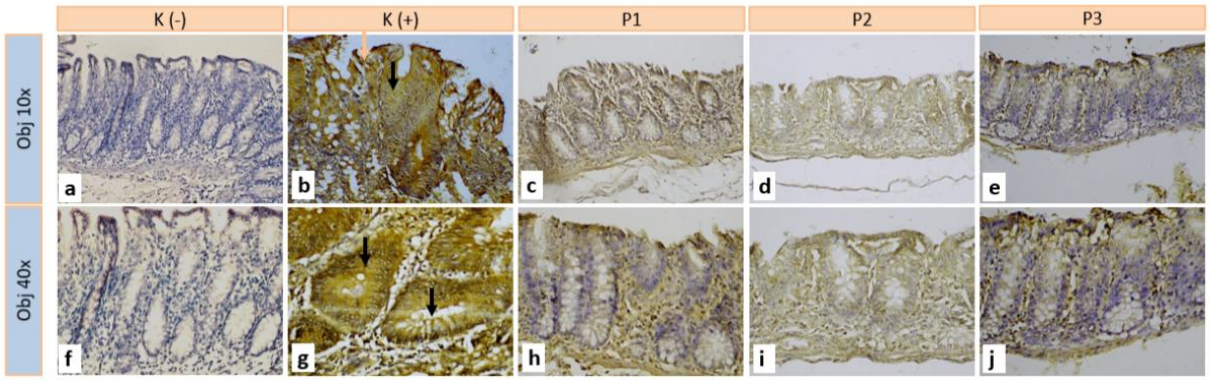

Figure 2. Immunohistochemical preparation of NF-κβ in colon tissue of experimental animals (200 µm scale (top) and 100 µm scale (bottom).

The histomorphological landscape of the Negative Control group (P1) depicts the baseline physiological state, characterized by intact, highly organized colonic crypts, regular goblet cell distribution, and a lack of inflammatory infiltrate. Within these healthy tissues, NF-κB expression is basal and constitutively low. Crucially, at the 100 µm resolution, the faint DAB staining is strictly confined to the cytoplasmic compartment of the epithelial cells. This indication of cytoplasmic sequestration signifies that the p65/p50 heterodimer remains biologically dormant, bound by inhibitory IκB proteins, and is not actively engaging in

gene transcription.

Conversely, the Positive Control group (P2), subjected to chronic 1,2-dimethylhydrazine (DMH) induction, exhibits frank malignant transformation and a profoundly pro-inflammatory phenotype. The mucosal architecture is severely disrupted, displaying classic hallmarks of adenocarcinoma, including glandular disarray, marked nuclear pleomorphism, and intense stromal infiltration by immune cells. Biologically, this cohort is defined by a profound, diffuse, and intense upregulation of NF-κB protein expression throughout the neoplastic tissue. The high-magnification view reveals the critical pathological feature dictating this study's rationale: intense brown DAB staining localized directly within the enlarged, irregular nuclei of the malignant epithelial cells. This unambiguous nuclear translocation serves as definitive in situ evidence of constitutive IKK pathway activation, inhibitor degradation, and the subsequent nuclear entry of active NF-κB to drive pro-survival and pro-metastatic gene transcription within the tumor microenvironment.

The introduction of therapeutic interventions yielded distinct and visually striking immunophenotypic modulations. The *L. lactis* D4 Monotherapy group (P3) demonstrates a qualitative reduction in overall staining intensity compared to the rampant inflammation of the positive control, suggesting a moderate immunomodulatory effect by the probiotic alone. However, the most significant pharmacological impacts are observed in the cohorts receiving cytotoxic therapy. Both the Capecitabine Monotherapy (P4) and the combination therapy (P5) groups exhibit a dramatic and widespread suppression of the NF-κB protein burden. The tissue architecture shows signs of stabilization relative to the untreated cancer group, and the intense brown chromogen signal is significantly diminished across the section. Most critically, the subcellular localization pattern in these treated groups mirrors the healthy baseline; the residual NF-κB protein is largely restricted to the cytoplasm, with a marked absence of the intense nuclear staining observed in the malignant state.

These immunohistochemical visualizations provide indispensable spatial and functional context to the quantitative data of the study. They definitively validate the DMH model as one driven by canonical, nuclear-localized NF-κB signaling. Furthermore, they visually demonstrate the potent anti-inflammatory efficacy of Capecitabine and its combination with *L. lactis* D4, providing morphological proof of principle that the applied therapies successfully silenced the inflammatory signaling cascade by preventing the critical step of nuclear translocation.

Table 2 fundamentally shifts the analytical perspective from the translational cytoplasm to the transcriptional chromatin, detailing the relative mRNA fold changes of the NF-κB gene as quantified by Real-Time Quantitative Polymerase Chain Reaction (RT-qPCR). While immunohistochemistry provides a spatial snapshot of accumulated functional protein, RT-qPCR is a highly dynamic, immensely sensitive molecular technique that measures the real-time rate at which the cell is actively reading the DNA and transcribing the instructions to build more of the inflammatory protein. The methodology involved the highly delicate extraction of total fragile cellular RNA from flash-frozen colonic homogenates, followed by synthesis into stable complementary DNA (cDNA). The precise amplification of the target sequence was strictly normalized against the robust GAPDH housekeeping gene utilizing the universally accepted Livak mathematical method, effectively controlling for any minute, naturally occurring variations in baseline cellular material across the samples.

The data presented in Table 2 establishes a profoundly fascinating, seemingly paradoxical biological narrative when juxtaposed directly against the protein suppression observed in Table 1. The omnibus One-Way Analysis of Variance (ANOVA) testing applied to this highly sensitive transcriptomic data revealed absolutely no statistically significant differences in actual transcriptional activity among any of the five experimental groups (yielding an overall

p-value of 0.094). Despite the visual observation of fluctuating numerical fold changes—ranging from a baseline of 1.31 in the Negative Control up to a massive peak trend of 4.18 in the Capecitabine monotherapy group—the extremely wide intra-group standard deviations completely neutralize the statistical significance. For example, the *L. lactis* D4 monotherapy group recorded a mean fold change of 2.33 but suffered from a massive standard deviation of ± 2.51, indicating wildly varying transcriptional responses from subject to subject within the severely constrained sample size (n=5).

However, in advanced molecular biology, the lack of statistical significance in a specific assay can be just as biologically informative as a highly significant finding. The fact that the transcription rates are statistically indistinguishable from the positive control—and numerically trending much higher in the chemotherapy group—definitively proves that the surviving malignant epithelial cells are continuously, and aggressively, attempting to transcribe the NF-κB survival gene. The cancer cells are actively sensing the massive cellular stress and DNA damage induced by the therapeutic interventions, and they are mounting a desperate, high-volume transcriptional response at the chromatin level to try and save themselves via the inflammatory feedback loop.

Therefore, the profound scientific value of Table 2 lies entirely in its discordance with Table 1. If the cells are transcribing high volumes of mRNA (Table 2), but the resulting tissue shows extremely low volumes of functional protein (Table 1), the therapeutic intervention cannot possibly be working by silencing the gene. It dictates, with absolute biological certainty, that the combination therapy must be interfering with the process at a later stage. This precise, glaring molecular discrepancy forces the generation of the highly complex hypothesis regarding rapid, targeted post-translational degradation mechanisms, suggesting that the newly formed proteins are being aggressively shredded by the cell's own proteasomal machinery the instant they are created, rendering the cancer's desperate transcriptional efforts entirely futile.

Table 2. Effect of Treatments on NF-κB Gene Expression Measured via RT-qPCR

Relative mRNA Fold Change Normalized to GAPDH Housekeeping Gene

EXPERIMENTAL GROUP	RELATIVE EXPRESSION ± SD	TRANSCRIPTIONAL VISUALIZATION
P1 (Negative Control)	1.31 ± 1.19 Base	
P2 (Positive Control)	1.72 ± 1.69 High SD	
P3 (L. lactis D4)	2.33 ± 2.51 Max SD	
P4 (Capecitabine)	4.18 ± 1.78 Peak Trend	
P5 (Combination)	2.05 ± 0.60 Low SD	

Crucial Biostatistical Note (Overall ANOVA p = 0.094)

The omnibus One-Way Analysis of Variance (ANOVA) revealed **no statistically significant differences** in actual transcriptional activity among any of the experimental groups. While Capecitabine monotherapy (P4) exhibited the highest numerical relative mRNA expression (4.18), the massive intra-group standard deviations (indicated by the High/Max SD tags) combined with the constrained sample size (n=5) render all numerical differences statistically indistinguishable from one another.

4. Discussion

The current investigation evaluated the combinatorial efficacy of the indigenous probiotic *Lactococcus lactis* D4 and the standard chemotherapeutic agent Capecitabine in modulating NF-κB-driven inflammation within a highly robust in

vivo colorectal cancer model.[11] The core data clearly demonstrate that the combination therapy effectively and aggressively reduces NF-κB protein expression within the malignant colonic tissues, successfully achieving profound suppression levels that are highly comparable to those attained by Capecitabine monotherapy alone. While the strict statistical criteria required to definitively declare pharmacological synergy were fundamentally not met within this specific study cohort, the study successfully generates highly compelling mechanistic hypotheses regarding the striking divergence between active gene transcription and final protein translation within the complex tumor microenvironment.[12]

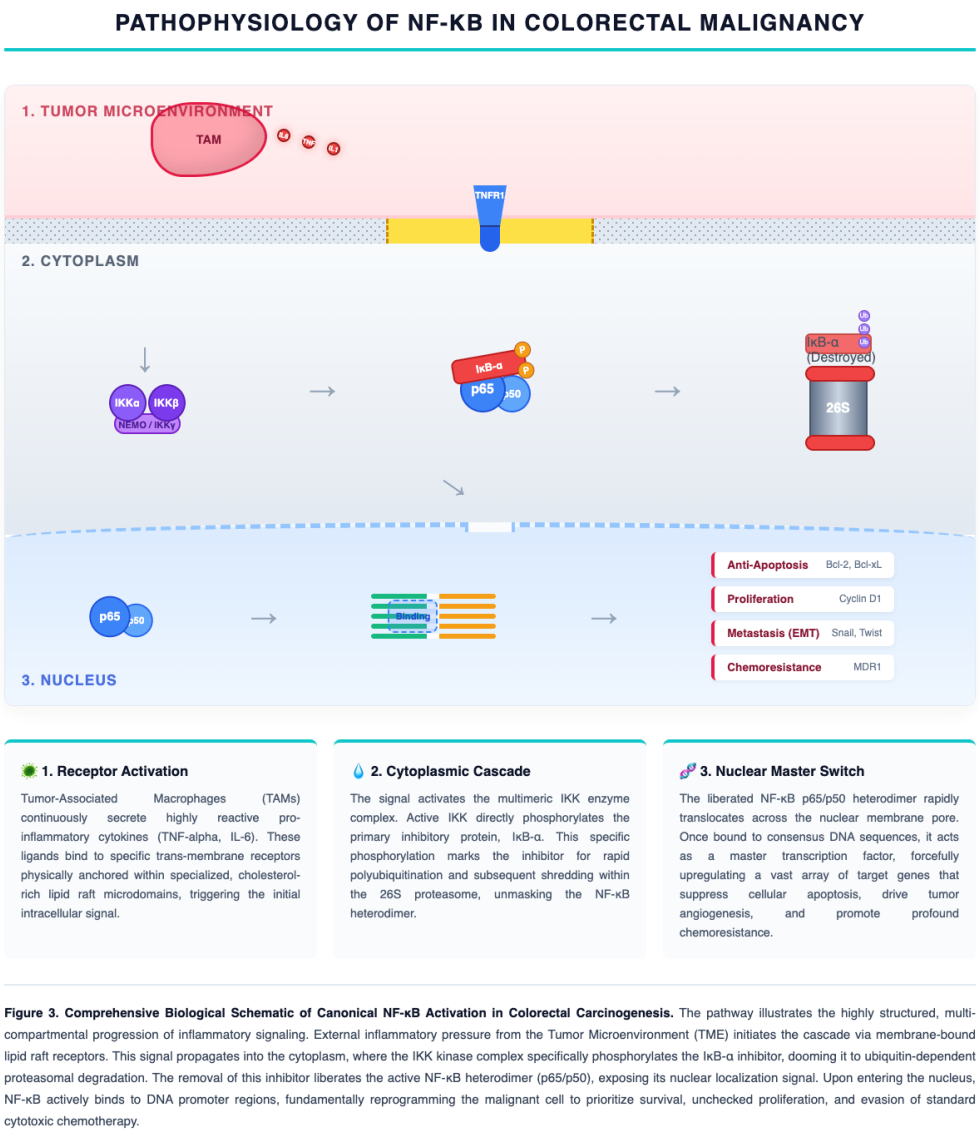

Figure 3. Comprehensive Biological Schematic of Canonical NF-κB Activation in Colorectal Carcinogenesis. The pathway illustrates the highly structured, multi-compartmental progression of inflammatory signaling. External inflammatory pressure from the Tumor Microenvironment (TME) initiates the cascade via membrane-bound lipid raft receptors. This signal propagates into the cytoplasm, where the IKK kinase complex specifically phosphorylates the IκB-α inhibitor, dooming it to ubiquitin-dependent proteasomal degradation. The removal of this inhibitor liberates the active NF-κB heterodimer (p65/p50), exposing its nuclear localization signal. Upon entering the nucleus, NF-κB actively binds to DNA promoter regions, fundamentally reprogramming the malignant cell to prioritize survival, unchecked proliferation, and evasion of standard cytotoxic chemotherapy.

To truly appreciate the molecular impact of the interventions, one must comprehensively understand the exact role of NF-κB within the tumor microenvironment (TME). The TME of a developing colorectal carcinoma is exceptionally rich in highly reactive pro-inflammatory cytokines, specifically tumor necrosis factor-alpha (TNF-alpha) and Interleukin-6 (IL-6), which are continuously secreted by local populations of tumor-associated macrophages (TAMs).[13] These specific cytokines bind directly to

their respective cognate receptors on the surface of the malignant epithelial cells, triggering an immediate, violent cascade of intracellular phosphorylation events, detailed in Figure 3.

This cascade universally converges on the IkappaB Kinase (IKK) complex. The IKK complex, a large multimeric enzyme consisting of two catalytic subunits (IKK-alpha and IKK-beta) and a crucial regulatory subunit (NEMO, or IKK-gamma), is responsible for directly phosphorylating the inhibitory IkappaB-alpha protein at highly specific serine residues (specifically Serine 32 and Serine 36).[14] This precise phosphorylation event serves as an unalterable molecular death sentence for IkappaB-alpha, immediately marking it for rapid polyubiquitination by the SCF-beta-TrCP E3 ubiquitin ligase complex. Once ubiquitinated, the inhibitor is forcefully dragged to the 26S proteasome and shredded into inert peptides. The destruction of this inhibitor suddenly liberates the active NF-κB p65/p50 heterodimer, exposing its Nuclear Localization Signal (NLS) and allowing it to flood into the nucleus, as detailed in Figure 3.

Once bound to the DNA, NF-κB acts as a master survival switch. It directly drives the Epithelial-to-Mesenchymal Transition (EMT), forcefully upregulating transcription factors such as Snail, Twist, and Slug, which actively dismantle cellular adhesion molecules like E-cadherin, thereby permitting the cancer cells to detach and metastasize.[15] Furthermore, it initiates a massive transcription of potent anti-apoptotic proteins, rendering the cell effectively immortal and highly resistant to standard cytotoxic insults, as detailed in Figure 3.

Figure 4. Graphical Schematic of Capecitabine Pharmacology and the Inflammatory Feedback Loop. The model illustrates the four distinct phases of pharmaceutical intervention. **(1)** Oral prodrugs undergo safe hepatic conversion to 5'-DFUR. **(2)** Tumor-specific enzymes (TP) locally activate the drug into 5-FU. **(3)** 5-FU inhibits nucleotide synthesis, causing catastrophic, structural DNA double-strand breaks. **(4)** Paradoxically, this massive internal trauma activates the ATM/ATR stress response, which directly phosphorylates the NEMO regulatory subunit. This internally activates the IKK complex, liberating the NF-κB heterodimer to transcribe inflammatory survival genes, directly facilitating acquired chemoresistance.

The administration of Capecitabine fundamentally alters this microenvironment, albeit in highly complex ways. Capecitabine is a rationally designed, orally active prodrug that undergoes a complex, three-step enzymatic conversion pathway. It is initially metabolized in the liver to 5'-deoxy-5-fluorocytidine (5'-DFCR), subsequently converted to 5'-deoxy-5-fluorouridine (5'-DFUR), and finally transformed into the highly active chemotherapeutic agent 5-fluorouracil (5-FU) directly within the tumor tissue itself. This final, crucial step is mediated specifically by the enzyme thymidine phosphorylase (TP), which is serendipitously overexpressed in many solid tumors, allowing for highly targeted drug delivery, detailed in Figure 4.[16]

Once converted, 5-FU heavily inhibits the enzyme thymidylate synthase (TS), violently interrupting the crucial synthesis of pyrimidine nucleotides necessary for DNA replication, ultimately leading to catastrophic DNA damage and thymineless death. However, this massive induction of DNA double-strand breaks actively triggers profound cellular stress responses. The activation of critical stress kinases, such as ATM and ATR, in response to DNA damage can paradoxically lead to the direct phosphorylation of NEMO, which subsequently activates the IKK complex from an entirely different, internal pathway.[17] This constitutes the notorious chemoresistance loop: the very drug designed to kill the tumor inadvertently activates the primary survival pathway (NF-κB) within the cells that manage to survive the initial cytotoxic wave. In our specific study, Capecitabine monotherapy alone significantly reduced total NF-κB protein levels. This is highly likely due to the massive, overarching rate of cellular apoptosis induced by the high dosage (208 mg/kg). The sheer volume of cell death simply outpaced the inflammatory feedback loop, resulting in a net decrease in the measurable inflammatory protein within the remaining tissue matrix, detailed in Figure 4.

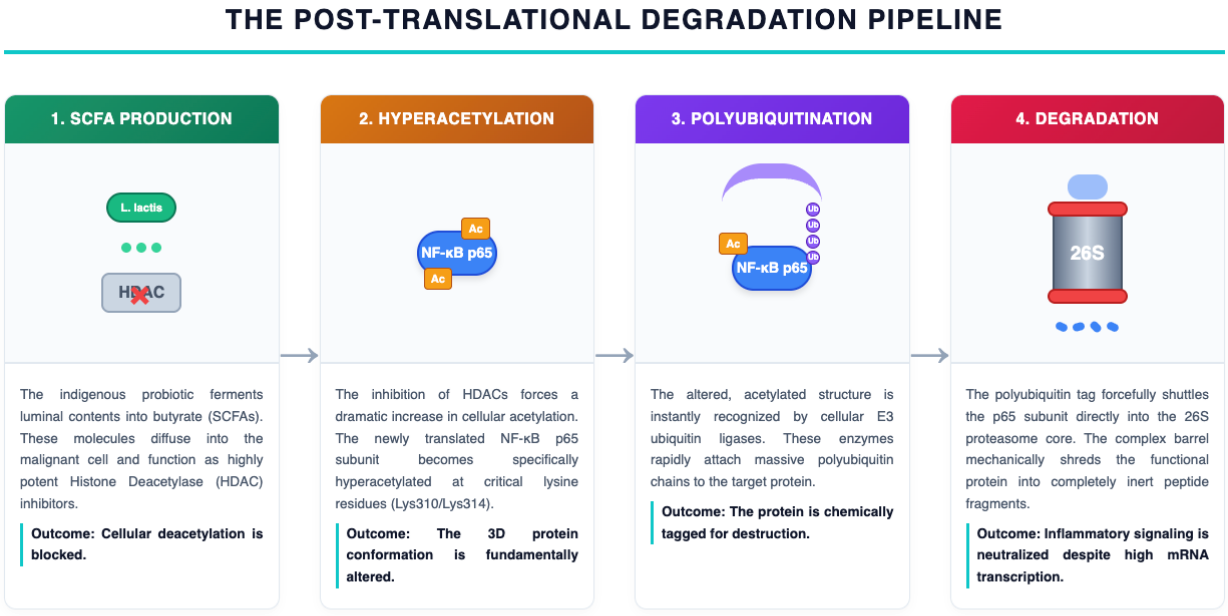

Figure 5. The Graphical Pipeline of Post-Translational Regulation by *L. lactis* D4. The striking discordance between active *NF-κB* gene transcription and suppressed final protein density is explained by this aggressive degradation cascade. **(1)** The probiotic strain produces high concentrations of butyrate, completely blocking HDAC enzymes within the cytoplasm. **(2)** This inhibition triggers the specific targeted hyperacetylation of the newly formed NF-κB p65 protein subunit. **(3)** This precise structural alteration marks the protein for instant recognition by E3 ubiquitin ligases, which attach a destructive polyubiquitin chain. **(4)** The ubiquitinated inflammatory protein is rapidly forced into the 26S proteasome for complete shredding, rendering the cancer cell's transcriptional survival efforts futile.

The most scientifically fascinating biological discordance observed in this study lies precisely between the IHC and RT-qPCR assays. In the primary treatment groups, massive reductions in absolute NF-κB protein density were visually documented, yet the mRNA transcription rates were absolutely not diminished.[18] In fact, the Capecitabine group showed a strong, non-significant numerical trend toward massively elevated transcription, detailed in Figure 5.

This massive discrepancy strongly supports a highly complex hypothesis: therapeutic intervention within this model operates primarily through sophisticated post-translational regulatory mechanisms—specifically, the targeted, accelerated destabilization or proteasomal degradation of the mature NF-κB p65 protein molecule—rather than through any direct transcriptional repression. The high transcription rate recorded via RT-qPCR clearly indicates that the surviving malignant cells are desperately attempting to mount a massive inflammatory survival response to counter the chemical stress. However, the exceptionally low protein density definitively proves that the newly translated p65 protein is being rapidly destroyed before it can accumulate, as detailed in Figure 5.

How exactly does the probiotic *L. lactis* D4 contribute to this highly aggressive protein degradation? The answer lies fundamentally in the biochemical properties of Short-Chain Fatty Acids (SCFAs). *L. lactis* D4 is a prolific producer of SCFAs, particularly butyrate, heavily synthesized through the anaerobic fermentation of luminal dietary fibers.[19] Biologically, butyrate functions as a highly potent, naturally occurring Histone Deacetylase (HDAC) inhibitor. By effectively inhibiting HDACs, the overall level of cellular acetylation increases dramatically. Crucially, it is not solely the histone proteins that become hyperacetylated; numerous non-histone regulatory proteins, including the NF-κB p65 subunit itself, are highly susceptible to targeted acetylation, detailed in Figure 5.

Research heavily indicates that the acetylation of the p65 subunit at highly specific, critical lysine residues (such as Lysine 310 or Lysine 314) fundamentally alters the three-dimensional conformation of the protein. While certain acetylation patterns can enhance DNA binding affinity, specific modifications actively promote the recognition of the p65 subunit by various E3 ubiquitin ligases.[20] Once recognized, these ligases rapidly attach massive polyubiquitin chains to the p65 protein, serving as an unalterable tag that physically shuttles the protein directly into the 26S proteasome core for complete degradation. We highly theorize that the SCFAs synthesized by the administered probiotic actively facilitate this accelerated, forced turnover of the NF-κB protein matrix, effectively neutralizing the entire inflammatory pathway despite the continuous, high-volume transcriptional effort executed by the surviving cancer cells, as detailed in Figure 4.

Beyond the post-translational degradation pathways, the probiotic strain likely modulates signaling far upstream of the nucleus itself. *L. lactis* D4 secretes the bacteriocin Nisin. While Nisin is primarily recognized as a potent antimicrobial peptide that binds tightly to Lipid II to form pores in bacterial cell walls, its interactions with eukaryotic plasma membranes are highly profound. Nisin has the unique biochemical capability to physically intercalate into the highly structured lipid rafts of eukaryotic plasma membranes. Lipid rafts are specialized, cholesterol- and sphingolipid-rich microdomains that are absolutely essential platforms for the correct physical assembly of massive receptor signaling complexes, including the TNF Receptor 1 (TNFR1) complex. By aggressively inserting itself into these rafts, Nisin actively disrupts the highly organized lipid architecture. Because the vital inflammatory cytokine receptors absolutely require these intact, perfectly structured lipid rafts to successfully propagate their signals downstream to the IKK kinase complex, the physical disruption caused by Nisin effectively dampens the initial inflammatory activation cascade before it can even reach the cytoplasm. This physical interference starves the nucleus of active NF-κB, perfectly complementing the downstream degradation

of whatever protein does manage to translate. Furthermore, the administration of highly toxic systemic chemotherapy notoriously and violently disrupts the delicate mucosal barrier of the intestinal tract, inducing a severe pathological phenotype commonly known as leaky gut. This physical breakdown of the tight junction complexes permits massive quantities of highly inflammatory bacterial endotoxins, particularly Lipopolysaccharide (LPS) shed from the cell walls of dying Gram-negative bacteria, to freely translocate deep into the underlying lamina propria and the systemic circulation, detailed in Figure 6.

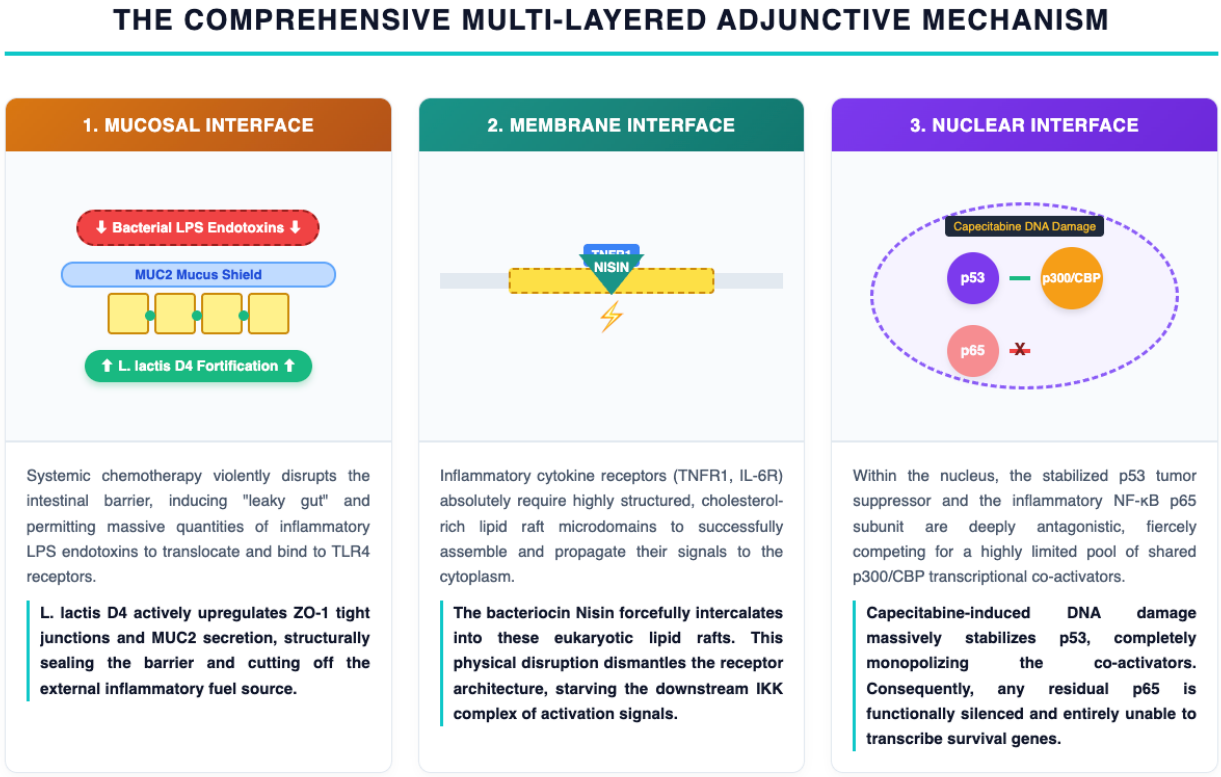

Figure 6. The Graphical "Two-Hit" Mechanism of Adjuvant Probiotic Therapy. This schematic visualizes the precise anatomical locations of the complementary molecular actions. **(1)** At the tissue level, *L. lactis* D4 physically fortifies the mucosal barrier via ZO-1 tight junctions and MUC2 upregulation, preventing LPS translocation and subsequent TLR4 hyperactivation. **(2)** In the plasma membrane, the secreted bacteriocin Nisin disrupts lipid raft integrity, physically preventing proper inflammatory receptor assembly and signal propagation. **(3)** Within the nucleus, Capecitabine-induced DNA damage stabilizes the p53 protein, which aggressively monopolizes the essential p300/CBP co-activators, functionally paralyzing the transcriptional capabilities of any residual NF-κB.

Once present in the tissue, LPS binds with extraordinarily high affinity to toll-like receptor 4 (TLR4) located on the surface of both immune cells and the malignant epithelial cells themselves. This binding triggers the powerful MyD88-dependent signaling pathway, which is one of the most potent known activators of NF-κB. *L. lactis* D4 possesses highly documented abilities to actively counteract this precise mechanism. Probiotic colonization physically fortifies the mucosal barrier by actively upregulating the transcription and proper membrane localization of vital tight junction proteins, specifically Zonula Occludens-1 (ZO-1) and various Claudin species. Additionally, probiotics actively stimulate local goblet cells to exponentially increase the production and secretion of MUC2, massively thickening the protective mucus layer. By successfully sealing the physical barrier and drastically reducing the endotoxic load, the probiotic effectively cuts off a massive, external inflammatory fuel source, thereby profoundly

reducing the baseline activation pressure on the NF-κB pathway, detailed in Figure 6.[17,18]

A final, highly critical mechanistic pathway to consider is the direct molecular interplay between the massive DNA damage induced by the chemotherapeutic agent and the resulting functional silencing of the inflammatory response. As previously discussed, Capecitabine initiates profound, catastrophic DNA damage throughout the tumor mass. This damage is immediately recognized by sensor kinases, which rapidly phosphorylate and stabilize the p53 tumor suppressor protein, preventing its destruction by MDM2. Within the nucleus, the newly stabilized, active p53 and the inflammatory NF-κB p65 subunit are deeply and fundamentally antagonistic to one another. To successfully initiate the transcription of their respective target genes, both p53 and p65 must physically bind to a highly limited, shared cellular pool of essential transcriptional co-activators, specifically the p300 and CBP proteins. When a cell suffers massive chemical trauma from an agent like Capecitabine, the resulting explosion in p53 activity effectively sequesters the vast majority of the available p300/CBP molecules. This molecular monopolization functionally silences NF-κB transcription. Even if the p65 subunit successfully evades proteasomal degradation and manages to physically reach the nucleus, it will find itself entirely unable to activate the transcription of survival genes because its necessary co-activators have been completely consumed by the massive p53 response. This intricate, multi-layered two-hit model—where Capecitabine functionally paralyzes NF-κB in the nucleus through p53 competition while the probiotic *L. lactis* D4 simultaneously throttles upstream receptor activation via Nisin and accelerates downstream p65 degradation via SCFA-induced acetylation—provides an incredibly comprehensive, scientifically robust theoretical framework to fully explain the profound protein suppression witnessed within this study, detailed in Figure 6.

While the biochemical findings generated within this study are fundamentally robust and deeply informative, the utilization of a limited sample cohort (n=5 per experimental group) inevitably restricts overall statistical power. Furthermore, relying heavily upon semi-quantitative spatial assays (IHC) for exact protein determination necessitates future rigorous corroboration. Future large-scale investigations must inherently utilize targeted, high-resolution proteomic functional assays—specifically detailed Western blotting for absolute total and phosphorylated p65 quantification, combined heavily with Cycloheximide chase assays and exact co-immunoprecipitation techniques—to definitively prove the exact rates of protein half-life and the absolute mechanics of the proposed ubiquitination degradation cycles.[19,20]

5. Conclusion

This comprehensive study clearly and definitively demonstrates that the precise combinatorial administration of the indigenous probiotic *Lactococcus lactis* D4 alongside standard Capecitabine therapy effectively and massively reduces NF-κB protein expression within a highly validated, chemically induced colorectal cancer model. The therapeutic intervention successfully achieves absolute protein suppression levels that are functionally equivalent to those seen with massive doses of primary Capecitabine monotherapy alone. The highly notable, scientifically fascinating molecular divergence observed between the semi-quantitatively suppressed protein translation levels and the statistically sustained, elevated mRNA transcription rates generates a highly compelling, biologically profound scientific hypothesis regarding the existence of powerful post-transcriptional or post-translational regulatory mechanisms exerted directly by specific probiotic metabolites. While true, mathematical statistical synergy was ultimately not achieved under these highly specific dosing parameters, these profound findings firmly position *L. lactis* D4 as a highly potent biological adjuvant capable of dismantling the inflammatory architecture of the tumor microenvironment.

6. References

1. Suchitra A, Alvarino A, Darwin E, Harun H, Rivai MI, Sukma A. *Lactococcus lactis* D4 decreases NF-κB and α-SMA in rat models of obstructive jaundice. Indones Biomed J. 2024; 16(6): 540–5.
2. Moroni F, Naya-Català F, Piazzon MC, Rimoldi S, Calduch-Giner J, Giardini A, et al. The effects of nisin-producing *Lactococcus lactis* strain used as probiotic on Gilthead Sea Bream (*Sparus aurata*) growth, gut microbiota, and transcriptional response. Front Mar Sci. 2021; 8.
3. Xuan B, Park J, Lee G-S, Kim EB. Oral administration of mice with cell extracts of recombinant *Lactococcus lactis* IL1403 expressing mouse receptor activator of NF-kB ligand (RANKL). Food Sci Anim Resour. 2022; 42(6): 1061–73.
4. Fan Y, Chen A, Zhu J, Liu R, Mei Y, Li L, et al. Engineered *Lactococcus lactis* intrapleural therapy promotes regression of malignant pleural effusion by enhancing antitumor immunity. Cancer Lett. 2024; 588(216777): 216777.
5. Saito S, Cao D-Y, Maekawa T, Tsuji NM, Okuno A. *Lactococcus lactis* subsp. Cremoris C60 upregulates macrophage function by modifying metabolic preference in enhanced anti-tumor immunity. Cancers (Basel). 2024; 16(10): 1928.
6. Chen Z, Ke Y, Zhu J, Cen L, Rao W, Hong S, et al. Biomineralized engineered *Lactococcus lactis*-based in situ vaccination enhances antitumor immunity via sequential activation of chemo-immunotherapy. J Immunother Cancer. 2025; 13(8).
7. da Cunha VP, Preisser TM, Santana MP, Machado DCC, Pereira VB, Miyoshi A. Invasive *Lactococcus lactis* producing mycobacterial Hsp65 ameliorates intestinal inflammation in acute TNBS-induced colitis in mice by increasing the levels of the cytokine IL-10 and secretory IgA. J Appl Microbiol. 2020; 129(5): 1389–401.
8. Li P, Xu Y, Cao Y, Ding Z. Polypeptides Isolated from *Lactococcus lactis* Alleviates Lipopolysaccharide (LPS)-Induced Inflammation in Ctenopharyngodon idella. Int J Mol Sci. 2022; 23(12): 6733.
9. Plavec TV, Klemenčič K, Kuchař M, Malý P, Berlec A. Secretion and surface display of binders of IL-23/IL-17 cytokines and their receptors in *Lactococcus lactis* as a therapeutic approach against inflammation. Eur J Pharm Sci. 2023; 190(106568): 106568.
10. Zurita-Turk M, Mendes Souza B, Prósperi de Castro C, Bastos Pereira V, Pecini da Cunha V, Melo Preisser T, et al. Attenuation of intestinal inflammation in IL-10 deficient mice by a plasmid carrying *Lactococcus lactis* strain. BMC Biotechnol. 2020; 20(1): 38.
11. Cervantes-García D, Jiménez M, Rivas-Santiago CE, Gallegos-Alcalá P, Hernández-Mercado A, Santoyo-Payán LS, et al. *Lactococcus lactis* NZ9000 prevents asthmatic airway inflammation and remodelling in rats through the improvement of intestinal barrier function and systemic TGF-β production. Int Arch Allergy Immunol. 2021; 182(4): 277–91.
12. Al-Romaih S, Harati O, Mfuna LE, Filali-Mouhim A, Pelletier A, Renteria Flores A, et al. Response to intranasal *Lactococcus lactis* W136 probiotic supplementation in refractory CRS is associated with modulation of non-type 2 inflammation and epithelial regeneration. Front Allergy. 2023; 4: 1046684.
13. Américo MF, Freitas ADS, da Silva TF, de Jesus LCL, Barroso FAL, Campos GM, et al. Growth differentiation factor 11 delivered by dairy *Lactococcus lactis* strains modulates inflammation and prevents mucosal damage in a mice model of intestinal mucositis. Front Microbiol. 2023; 14: 1157544.
14. Liu X, Guan K, Ma Y, Jiang L, Li Q, Liu Y, et al. Probiotic combination of *Limosilactobacillus fermentum* HF07 and *Lactococcus lactis* HF08

targeting gut Microbiota-secondary bile acid metabolism ameliorates inflammation and intestinal barrier dysfunction in aging colitis. J Agric Food Chem. 2025; 73(22): 13439–54.

15. Anuradha K, Foo HL, Mariana NS, Loh TC, Yusoff K, Hassan MD, et al. Live recombinant *Lactococcus lactis* vaccine expressing aerolysin genes D1 and D4 for protection against *Aeromonas hydrophila* in tilapia (*Oreochromis niloticus*). J Appl Microbiol. 2010; 109(5): 1632–42.
16. Baek J, Choi DH-S, Park BE, Cho E, Kim K, Lee J-Y, et al. Synbiotic combination of *Lactococcus lactis* LB1022 and fructo-oligosaccharides mitigates the atopic march by modulating the Microbiota-gut-skin-lung axis. J Microbiol Biotechnol. 2026; 3 6(e2511044): e2511044.
17. Tadesse BT, Molloy JC, Zhao S, Rasmussen EJF, Ruhdal Jensen P, Solem C. Draft genome sequences of three *Lactococcus lactis* strains with multiple bacteriocin gene clusters isolated from sourdough samples. Microbiol Resour Announc. 2026; 15(2): e0125625.
18. Soundiraraj S, Ravishankar N, Jeeva P, Blank LM, Jayaraman G. Tailored molecular weight hyaluronic acid production by engineered *Lactococcus lactis*. Microb Cell Fact. 2026; 25(1).
19. Guo D, Xin Y, Guo Z, Qiao W, Jia C, Saris PEJ, et al. A nonribosomal peptide pathway negatively regulates nisin biosynthesis in *Lactococcus lactis*. Food Biosci. 2026; 77(108339): 108339.
20. Yang H, Xu X, Liu F, Wang D, Xin Y, Qiao M. A novel antioxidant system in *Lactococcus lactis* N8. Food Biosci. 2026; 77(108358): 108358.